

The minimum dry mass is about 0.3% less than with a single-position nozzle. For two-stage systems, a single expansion ratio of 77.5 provides a lower dry mass than any two-position nozzle.

The nozzle characteristics are based on regenerative cooling of the nozzle extension. If a radiation-cooled nozzle could be used, the nozzle would have a lower mass, and higher expansion ratios would provide minimum dry weight.

### Appendix

The equation for vacuum specific impulse,  $I_{sp}$ , is

$$I_{sp} = a(e/60)^b$$

where  $e$  is the expansion ratio,  $a$  is 450.5 s, and  $b$  is 0.004375 for expansion ratios less than 60 and 0.02945 for expansion ratios greater than 60. This equation represents the data as accurately as could be read from the provided curves. It applies only to the case considered in which the engine powerhead is held constant and only the nozzle expansion ratio is varied.

The engine mass  $m$  is first calculated in English units because the information supplied by the manufacturer was provided in English units. The first step is to calculate the mass from

$$m = ce + d$$

where  $c$  is 17.76 lb and  $d$  is 6768 lb. This equation fits the linear curve provided by the manufacturer. It gives the mass for an engine with a single expansion ratio and a vacuum thrust of 600,000 lb. This mass is then scaled to match the SSME mass of 3123 kg by multiplying by 3123 kg and dividing by  $m$  for  $e = 77.5$ . The mass at the thrust level required for the sized vehicle is found by multiplying by the required vacuum thrust and dividing by the SSME thrust of 2293.1 kN. The mass calculated in this manner is correct for a single-position nozzle. For a two-position nozzle, the same mass is correct if the higher expansion ratio is used and a mechanism mass is added.

For a two-position nozzle, the mechanism mass  $r$  is calculated from

$$r = f(e^{0.5} - 1)p$$

where  $f$  is 0.0455 s and  $p$  is the propellant flow rate, which can be calculated by the thrust divided by the specific impulse and, for  $r$  in mass units, by the acceleration of gravity. This equation was not derived from the recent data provided for this study. For the SSME at full power level and for an expansion ratio of 150, the mechanism mass is given by this equation to be 264 kg.

### Acknowledgment

The author wishes to express appreciation to Mr. Frank Kirby of the Rocketdyne Division, Rockwell International Corporation, for providing the data used to derive the engine specific impulse and mass equations without which this study could not have been accomplished.

### References

- <sup>1</sup>Martin, J. A., "Tripropellant Engines of Earth-to-Orbit Vehicles," *Journal of Spacecraft and Rockets*, Vol. 22, Nov.-Dec. 1985, pp. 620-625.
- <sup>2</sup>Martin, J., Naftel, J., and Turriziani, R., "Propulsion Evaluation for Orbit-on-Demand Vehicles," *Journal of Spacecraft and Rockets*, Vol. 23, Nov.-Dec. 1986, pp. 612-619.
- <sup>3</sup>Marting, J. A., "Cost Comparisons of Dual-Fuel Propulsion in Advanced Shuttles," *Journal of Spacecraft and Rockets*, Vol. 16, July-Aug. 1979, pp. 232-237.

## Shock Wave Asymmetry of Sphere Cones at Angles of Attack

S. L. Gai\*

University College, U. N. S. W., Australian Defence Force Academy, Canberra, Australia

### Introduction

AS was pointed out several years ago by Greenberg and Traugott,<sup>1</sup> in the case of flow over a blunted cone at an angle of attack, conditions exist where, depending on the Mach number and the cone angle, the shock layer (the region of flow confined between the shock wave and the body) on the windward side will be thicker than that on the leeward side. They further point out that it was Gonor<sup>2</sup> who postulated the existence of two types of flow for a circular cone at angle of attack in supersonic/hypersonic flow: a "normal" or "regular" regime in which the leeward shock layer is thicker than the windward shock layer and a "reversed" flow regime in which the opposite is true. The existence of these types of flow regimes was stated to be dependent on the Mach number of the flow and the effective semicone angle (see Fig. 1). Figure 1 is reproduced from Ref. 1. It must be pointed out in this context, however, that Gonor's<sup>2</sup> paper seems to contain some errors, viz. that the theoretical expression for the effective semicone angle  $\theta^*$  does not reproduce the theoretical curves for the larger semicone angles  $\theta_0$  as shown in his Fig. 1 at  $M = 4$ . This fact has also been alluded to by the "Reviewer's Comment" at the end of that paper. Be that as it may, existence of "regular" and "reversed" regimes seem to be confirmed by Greenberg and Traugott.<sup>1</sup> In the experimental situation,  $\theta^*$  may be defined as  $\theta_0 \pm \alpha$  where  $\alpha$  is the angle of attack of the cone.

Greenberg and Traugott further point out that this phenomenon is also true for spherically blunted cones, and they present a photograph in support of this conclusion. This short Note shows further evidence in support of their conclusion and adds the observation that this flow feature becomes quite prominent in hypersonic, high enthalpy streams.

### Experiments and Discussion of Results

Tests on a spherically blunted cone of semiangle 13 deg ( $\theta_0$ ) at various angles of attack  $\alpha$  were conducted in the Australian National University free-piston driven shock tunnel T3<sup>3</sup> with nitrogen as the test gas. The flow was generated by a conical nozzle with exit and throat diameters of 203 and 12.7 mm, respectively. The freestream was dissociated nitrogen with speeds ( $U_\infty$ ) varying between 6 and 8 km/s and a Mach number  $M_\infty$  of approximately 6. The corresponding reservoir enthalpies  $h_0$  ranged from 30-52 MJ/kg, respectively. Since the freestream was dissociated nitrogen, freestream flow conditions at the exit plane of the nozzle were calculated using a computer program based on the method of Lordi et al.<sup>4</sup> for nonequilibrium gas expansions.

Self-luminosity photographs, taken with a fast electro-mechanical shutter (speed  $\approx 800$  cm/s) especially developed for these experiments,<sup>5</sup> were used to study shock waves around the body. Some of these photographs are shown in Fig. 2. A considerable effort was spent to ensure that the observed shock shapes are caused by test gas only and not by helium

Received Aug. 3; revision received Oct. 24, 1988. Copyright © American Institute of Aeronautics and Astronautics, Inc., 1989. All rights reserved.

\*Senior Lecturer, Mechanical Engineering Department. Member AIAA.

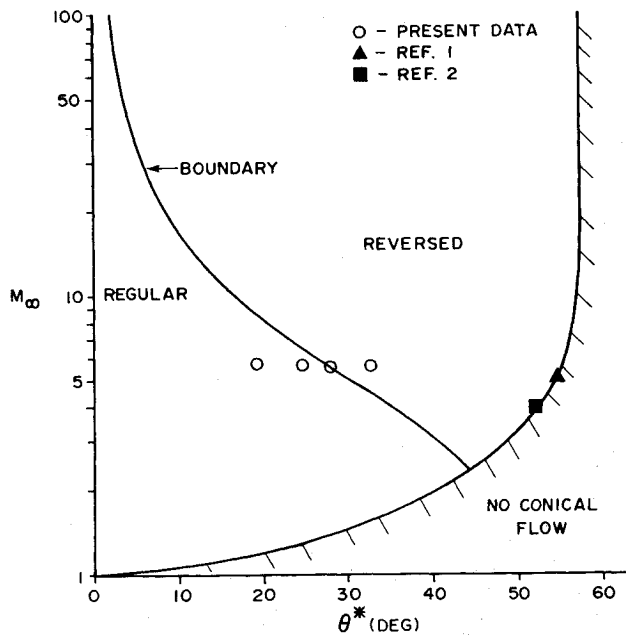
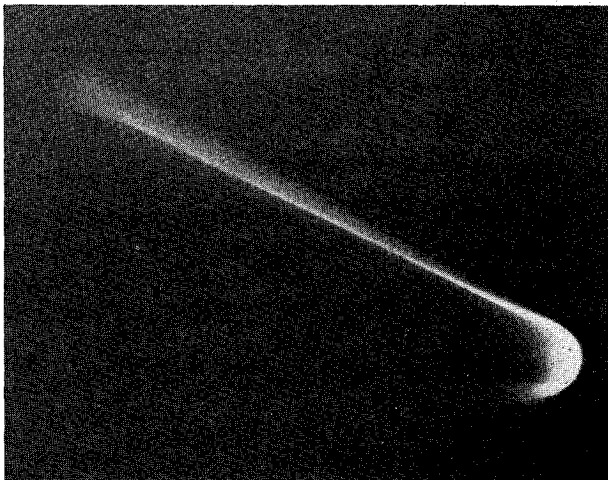


Fig. 1 Boundaries showing "regular" and "reversed" shock layer regimes.

(driver gas) contaminated test gas. The shutter developed was capable of being closed or opened during any part of the total run time so that photographs taken at various instances during the run could be compared and contamination effects avoided. Typically, the occlusion time was  $\sim 75 \mu\text{s}$  and the effective exposure time was  $150\text{--}200 \mu\text{s}$  in a run time of  $\sim 500 \mu\text{s}$ .

We note that, apart from the appearance of a shock inflection point, a phenomenon ascribed to the flow nonequilibrium effects in the nose region and discussed in Ref. 6, the windward shock layer becomes thicker with increasing angle of attack for a given enthalpy. Also to be noted is the thickness of the shock layer at a given enthalpy level. It will be seen also from the photographs that, because of very low density levels ( $\rho_\infty = 2 \times 10^{-3}$  to  $4 \times 10^{-3} \text{ kg/m}^3$ ), the leeward shock is not clearly visible. However, it can be made out that, as the angle of attack increases, it gets closer to the body surface. For the same reasons (i.e., low densities) and the slenderness of the cone, schlieren technique or interferometry was not sufficiently sensitive.

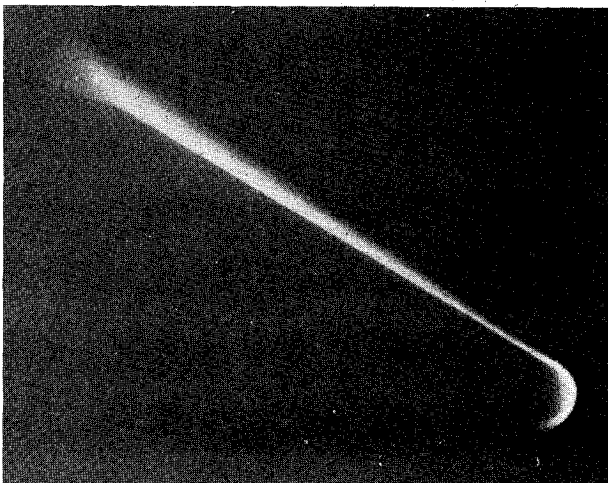
The results from Fig. 2 when plotted on Fig. 1 show that they straddle the two regimes with the higher angles of attack results being in the "reversed" flow regime. Also shown on Fig. 1 are the  $\theta_0 = 47.5 \text{ deg}$ ,  $\alpha = 7 \text{ deg}$ , and  $M_\infty = 5$  result quoted in Ref. 1 and the experimental result quoted by Gonor.<sup>2</sup>



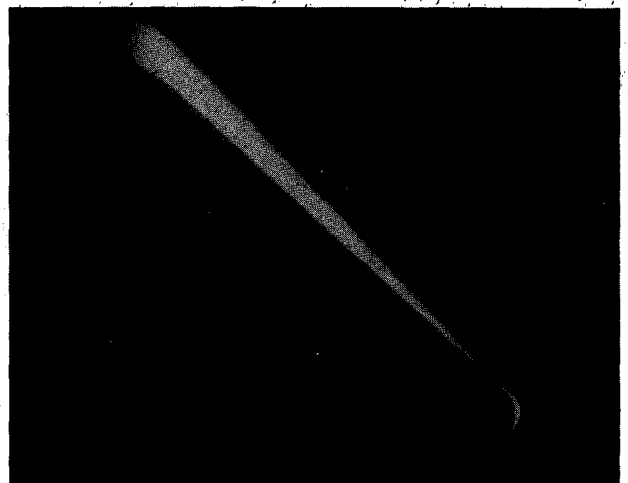
a)  $h_0 = 30 \text{ MJ/kg}$ ,  $\alpha = 6 \text{ deg}$



c)  $h_0 = 30 \text{ MJ/kg}$ ,  $\alpha = 15 \text{ deg}$



b)  $h_0 = 52 \text{ MJ/kg}$ ,  $\alpha = 12 \text{ deg}$



d)  $h_0 = 52 \text{ MJ/kg}$ ,  $\alpha = 20 \text{ deg}$

Fig. 2 Windward shocks on a sphere-cone in nitrogen.

Taken together, these results show that a blunted cone at a sufficiently high angle of attack in hypersonic flow can exhibit the "reversed" flow regime with respect to the shock layer on the windward side. It seems possible that, in addition, the effect of higher enthalpy stream is such as to enhance this feature of the flow.

### Acknowledgment

Grateful acknowledgment is due to the Australian Research Grants Scheme for its financial support.

### References

<sup>1</sup>Greenberg, R. A. and Traugott, S. C., "Shock Wave Asymmetry for Cones and Sphere-Cones at Angle of Attack," *ARS Journal*, Vol.

31, June 1961, pp. 821-822.

<sup>2</sup>Gonor, A. L., "Location of Frontal Wave in Asymmetrical Flow of Gas at High Supersonic Speed over a Pointed Body," *ARS Journal*, Vol. 30, Sept. 1960, pp. 841-842 (Russian Supplement).

<sup>3</sup>Stalker, R. J., "Development of a Hyper Velocity Wind Tunnel," *The Aeronautical Journal*, Vol. 76, June 1972, pp. 374-384.

<sup>4</sup>Lordi, J. A., Mates, R. E., and Moselle, J. R., "Computer Program for Numerical Solution of Non-Equilibrium Expansions of Reacting Gas Mixtures," NASA CR-472, 1966.

<sup>5</sup>Lyons, P. R. A., Kilpin, D., and Gai, S. L., "A New High Speed Electro-Mechanical Shutter," *Journal of Physics E: Scientific Instruments*, Vol. 17, Jan. 1984, pp. 108-109.

<sup>6</sup>Gai, S. L., Sandeman, R. J., Lyons, P., and Kilpin, D., "Shock Shape over a Sphere-Cone in Hypersonic High Enthalpy Flow," *AIAA Journal*, Vol. 22, July 1984, pp. 1007-1010.

## *Recommended Reading from the AIAA Progress in Astronautics and Aeronautics Series . . .*



# **Thermal Design of Aeroassisted Orbital Transfer Vehicles**

*H. F. Nelson, editor*

Underscoring the importance of sound thermophysical knowledge in spacecraft design, this volume emphasizes effective use of numerical analysis and presents recent advances and current thinking about the design of aeroassisted orbital transfer vehicles (AOTVs). Its 22 chapters cover flow field analysis, trajectories (including impact of atmospheric uncertainties and viscous interaction effects), thermal protection, and surface effects such as temperature-dependent reaction rate expressions for oxygen recombination; surface-ship equations for low-Reynolds-number multicomponent air flow, rate chemistry in flight regimes, and noncatalytic surfaces for metallic heat shields.

**TO ORDER:** Write AIAA Order Department,  
370 L'Enfant Promenade, S.W., Washington, DC 20024  
Please include postage and handling fee of \$4.50 with all  
orders. California and D.C. residents must add 6% sales  
tax. All orders under \$50.00 must be prepaid. All foreign  
orders must be prepaid.

**1985 566 pp., illus. Hardback**  
**ISBN 0-915928-94-9**  
**AIAA Members \$49.95**  
**Nonmembers \$74.95**  
**Order Number V-96**